UV-Induced Degradation Rates of 1,3,5-Triamino-2,4,6-Trinitrobenzene (TATB)

Darren L. Williams,*,† James C. Timmons,‡ James D. Woodyard,‡ Ken A. Rainwater,§ James M. Lightfoot,† Ben R. Richardson,† Caroline E. Burgess,‡ and John L. Heh‡

BWXT Pantex LLC, P.O. Box 30020, Amarillo, Texas 79120, West Texas A&M University, Canyon, Texas 79016, and Texas Tech University, Lubbock, Texas 79409

Received: October 21, 2002; In Final Form: August 14, 2003

We report a 2.5-year study of the photolytic degradation of 1,3,5-triamino-2,4,6-trinitrobenzene (TATB) with variations in temperature, humidity, and illumination by fluorescent and UV light (254, 312, and 365 nm). The free-radical decomposition product was monitored with electron paramagnetic resonance (EPR). The EPR spectrum of the green powder allowed reliable quantitation with a single peak (FWHM = 29.1 G). The variations in humidity showed little effect in accelerating the degradation of TATB. The only significant temperature effect was noticed at −10 °C, where fewer radicals formed. The radical production rates at −10 °C were some of the highest measured, however, suggesting that the rates under other temperature conditions had slowed, perhaps as a result of extensive conversion of surface molecules to radical species. We show that a substantial amount of radicals can be generated with UV light, and work is ongoing to modify our EPR spectrometer so that TATB can be irradiated in the EPR cavity to measure the initial rates of radical formation.

I. Introduction

The development and use of insensitive high explosives (IHEs) greatly improved the safety, reliability, and longevity of many important weapons systems for the United States Departments of Energy and Defense. The most common IHE is 1,3,5-triamino-2,4,6-trinitrobenzene (TATB). This high explosive has excellent shock resistance and thermal stability.[1] It was first documented in 1981 that this explosive changes color from yellow to green upon irradiation.[2] Since then, intermittent research has tried to determine the identity of the green substance.

Sharma and Owens[3] experimented with shock- and UV-decomposed TATB. Their XPS measurements of the N 1s transitions showed a decrease in the nitrogen signal of the nitro groups, but no quantitative information was presented. In 1981, using electron paramagnetic resonance (EPR) spectroscopy, Britt and co-workers confirmed Cady's observation[2] that the photodegradation product of TATB is a free radical. Their experiments showed that the free-radical species persisted for periods longer than 2 years even when exposed to air at ambient temperature. They also reported that radical formation appeared to be a surface phenomenon and that a single radical species was formed. The past 20 years saw significant activity devoted to the identification of the radical.[4−8] No research group, however, has reported either the radical production rate or photolytic degradation kinetics. These items are important for an understanding of explosive lifetime prediction and are the subject of this study.

This study endeavored to (1) identify the factors (e.g., radiation, temperature, and humidity) that promote the degradation of TATB, (2) study the photochemical reaction kinetics, and (3) identify the degradation products. The first two items in this list are presented in this paper, leaving the third item to a later publication.

II. Experimental Section

General Conditions. BWXT Pantex, LLC synthesized and supplied the ultra fine (20-μm) TATB used in this study. In all experiments, the bright yellow powder was degraded at Texas Tech University in open Petri dishes, each holding about 50 g. The powders were stirred once a day Monday through Friday. Ambient room temperature was used as the 24 °C condition, and all temperatures were maintained at ±5 °C of the desired temperature. At each sampling period, a 1-g laboratory sample was removed from each of the Petri dishes. Nothing was ever added back into the Petri dishes. The laboratory samples were stored in amber vials at ambient temperature and humidity (nominally 30% RH in the Texas Panhandle) after removal from the experimental conditions. The Varian E-109 electron paramagnetic resonance spectrometer at West Texas A&M University was used to measure the free-radical content in the laboratory samples using an X-band bridge and resonator. The EPR measurements of the laboratory samples were typically obtained within 1 week of sample removal from the Petri dishes.

Experiment 1: Effects of UV/Visible Exposure, Temperature, and Humidity. A full factorial four-factor statistical design was used to test the effects of light, temperature, humidity, and time of exposure on free-radical production in TATB. The light had two levels: UV (365-nm, Fisher Scientific) and fluorescent (common fluorescent tube light). The temperature levels were ambient temperature (nominally 24 °C) and 50 °C. Relative humidity was tested at three levels: low (nominally 30% RH), medium (~54% RH using $Na_2Cr_2O_7 \cdot 2H_2O$), and high (~80% RH using KCl at 50° C and $ZnSO_4 \cdot 7H_2O$ at room temperature). The medium and high humidity levels were controlled by placing the saturated salt solutions in open beakers inside the degradation chambers (see Figure 1). Twelve Petri dishes of powder were exposed (one for each experimental condition), and laboratory samples were taken from

* To whom correspondence should be addressed. E-mail: dlwillia@pantex.com.
† BWXT Pantex LLC.
‡ West Texas A&M University.
§ Texas Tech University.

10.1021/jp027263v CCC: $25.00
Published on Web 10/11/2003

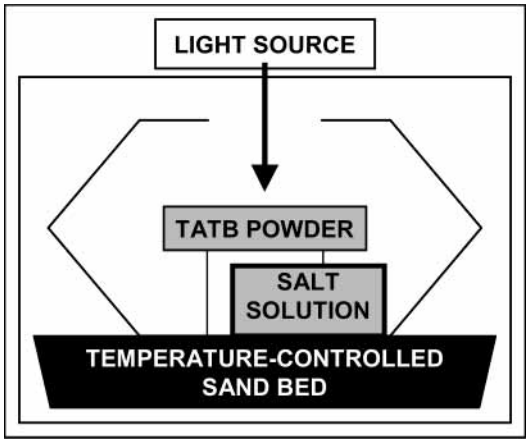

Figure 1. Degradation chambers used to control temperature and humidity.

the dishes at 3, 6, 9, and 12 months. A control sample was kept in the dark, at ambient temperature (~24 °C) in a dry container (~30% RH).

Experiment 2: Combined Effects of UV Exposure and Temperature. Experiment 2 was designed with three factors: UV wavelength, temperature, and time of exposure. Four different temperature levels were used: −10, 24, 50, and 75 °C. The −10 °C condition was obtained by placing the TATB into an upright freezer. Room temperature in the laboratory met the 24 °C temperature condition. The 50 and 75 °C conditions required a heated sand bed. Three UV lamps (Fisher Scientific) were used with wavelengths of 254, 312, and 365 nm. The lamps were mounted at appropriate distances above the TATB samples to deliver 1.4 mW/cm^2. Twelve Petri dishes of powder were used (one for each temperature−wavelength combination), and they were stirred 5 times per week to provide uniform UV exposure.

In experiment 2, copper(II) sulfate pentahydrate ($CuSO_4 \cdot 5H_2O$, Aldrich, 99.999% pure) was used as a calibration standard as described by Randolph.[9] The raw data were compared to the copper(II) sulfate pentahydrate calibration and are reported in terms of number of spins per gram of sample. The EPR spectra were taken at 119, 217, 314, 440, and 509 days for each environmental condition. The 1-g laboratory sample was divided into many (6−11) aliquots ranging in mass from 0.1 to 0.01 g. The range of masses was used for each sample to verify that the linear EPR response range was being used. Occasionally, the radical concentration was checked on some laboratory samples weeks after they were removed from the irradiation chambers, and all subsequent measurements were very close to the initial values (±2%).

It should be noted that we measured the samples differently in experiment 1 than in experiment 2. In the first experiment, the amount of sample was much larger than the magnetic sampling volume. This yielded a qualitative number of spins per sampling volume. It showed a substantial difference between the factors and served to guide the design of experiment 2. Also, the intensity of the light source at the sample was not measured in experiment 1, but it was less than the light intensity in experiment 2 because of the greater distance between source and sample.

III. Aging Results

General Results. The radicals produced a stable EPR peak of 29.1 G FWHM with no splitting, as seen in Figure 2. Double integration and calibration gave the number of spins per gram, and these results are shown for each experiment.

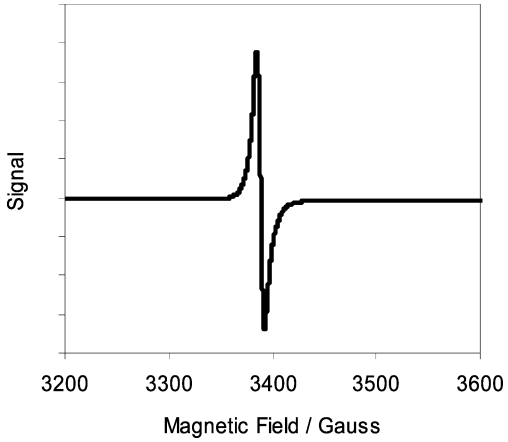

Figure 2. EPR spectrum of UV-irradiated TATB powder.

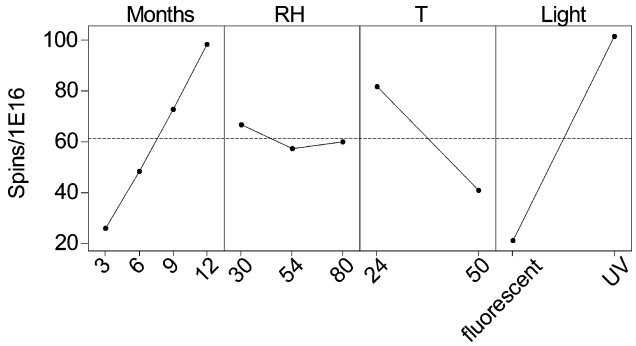

Figure 3. Factorial main effects plot of the four factors in experiment 1. The averages of all of the data at each level are plotted, and the connecting lines are meant to guide the eye.

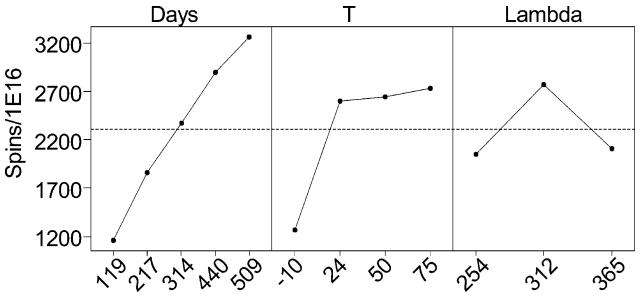

Figure 4. Factorial main effects plot of the three factors in experiment 2. The averages of all of the data at each level are plotted, and the connecting lines are meant to guide the eye.

Experiment 1: Effects of UV/Visible Exposure, Temperature, and Humidity. The data from experiment 1 are represented in Figure 3 by a factorial main effects plot. This statistical tool analyzes the changes in the level means to determine which factors influence the response the most.[10] The dashed horizontal line is the overall data mean. The labels across the top of the figure are the factors in the experiment. The labels across the bottom are the levels used for each factor. The plot has a common *y* axis and is divided horizontally by experimental factor. The averages of each level are plotted under each factor, and the connecting lines are meant to guide the eye to the factor with the greatest influence on radical production.

Experiment 2: Combined Effects of UV Exposure and Temperature. The factorial main effects plot of experiment 2 is shown in Figure 4. The mean of all data is shown by the horizontal dashed line, and the averages of the data at each level are plotted against a common *y* axis.

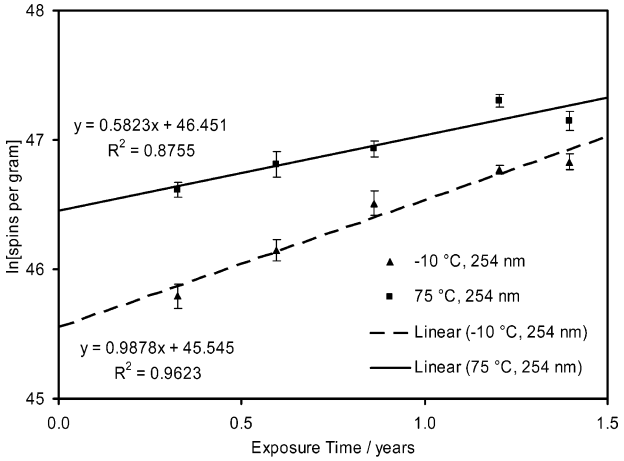

Figure 5. First-order kinetics of radical production under various conditions in experiment 2. Only 2 (highest and lowest k) of the 12 rate law curves are shown for clarity.

IV. Discussion

Experiment 1: Effects of UV/Visible Exposure, Temperature, and Humidity. The level means plotted in Figure 3 show that UV light has a strong effect on radical production. Florescent light produced very few radicals in comparison. The control was kept in a dark environment and did not give an EPR signal. There was also a very good response to time of exposure. The humidity variations had little effect on radical concentration. The samples exposed to 24 °C initially showed a higher radical concentration relative to the samples exposed to 50 °C. This temperature difference was observed only for the samples exposed to UV light, and upon closer inspection, it was discovered that a glass plate had been placed over the reaction container at the higher temperature to slow evaporation of the humidity-controlling salt solution. This had the unfortunate effect of filtering most of the UV light from the 50 °C, high-humidity reaction vessel. Nevertheless, any possible temperature dependence was studied in more detail in experiment 2.

Experiment 2: Combined Effects of UV Exposure and Temperature. It is clear from Figure 4 that cold temperature (−10 °C) retarded radical production. Analysis of variance does not show a statistical significance in the variations at 24, 50, and 75 °C. The variation related to UV wavelength was also insignificant at 95% confidence.

Linear least-squares analyses were performed on the radical concentrations for integrated rate laws[11] through order 3, and the R^2 values for all 12 conditions were highest for the first-order rate law given in eq 1. Note that the integrated rate law has a positive sign in front of the rate constant (k), indicating that the production of radicals, rather than the disappearance of reactant molecules, is being observed.

$$\ln[\text{radical}] = \ln[\text{radical}]_0 + kt \qquad (1)$$

Figure 5. shows 2 of the 12 plots of ln[radical] versus exposure time in years. These two cases were selected because they show the highest rate (0.99 ± 0.11 year^{-1}) and the lowest rate (0.58 ± 0.13 year^{-1}).

Table 1 shows the rates and the intercepts for all 12 combinations of UV wavelength and temperature. The intercepts $\ln[\text{radical}]_0$ in the table were converted to values of initial radical concentration ($[\text{radical}]_0$) in spins per gram. The rates computed from the least-squares analyses are low, and the intercepts are above our limit of quantitation 1.4×10^{19} spins per gram. These initial concentrations of radicals are high enough to be seen with the equipment in this study, and the control sample did not show any background radical content. Therefore, it is likely that the rates have slowed as a result of the high percent conversion after months of irradiation in experiment 2.

TABLE 1: Computed Radical Generation Rates and Initial Radical Concentrations under Different Conditions in Experiment 2

T (°C)	λ (nm)	$[\text{radical}]_0$[a] ($\times 10^{-19}$)	k[a] (year^{-1})
−10	254	6.0 (0.7)	0.99 (0.11)
24	254	9.0 (1.1)	0.94 (0.13)
50	254	14.1 (1.7)	0.77 (0.12)
75	254	14.9 (1.8)	0.58 (0.13)
−10	312	5.2 (0.8)	0.86 (0.16)
24	312	13.1 (1.6)	0.80 (0.13)
50	312	12.9 (2.2)	0.69 (0.18)
75	312	15.9 (0.8)	0.93 (0.05)
−10	365	5.3 (0.7)	0.97 (0.13)
24	365	10.8 (0.5)	0.88 (0.05)
50	365	10.6 (1.2)	0.93 (0.12)
75	365	11.7 (1.8)	0.68 (0.16)

[a] Values in parentheses give the standard deviations from the least-squares analysis.

It is interesting that the −10 °C conditions exhibited some of the highest production rates but the lowest absolute amounts of radical. This might be evidence that the rates have slowed in the 24, 50, and 75 °C samples. Using the molar mass of TATB (258.18 g/mol), one can see that 1 g of pure TATB contains 2.33×10^{21} molecules. Radical concentrations of 2×10^{20} spins per gram represent substantial percent conversions, and at these concentrations, all of the surface molecules likely have been converted to radicals. Therefore, the light must penetrate deeper into the particles to create more radicals. Two effects contribute to slowing of the rates of radical formation in subsurface molecules: (1) the absorption coefficient of UV light causes an attenuation of the photons penetrating below the surface to convert internal TATB molecules to radicals, and (2) the cage effect of radical pairs formed in an internal crystal lattice favors recombination. Ongoing work to irradiate fresh TATB in the EPR chamber will be forthcoming.

V. Conclusions

We have studied the photolytic degradation and radical production rates in TATB as a function of 24 different combinations of humidity, temperature, and illumination over 2.5 years. The variations in humidity showed little effect in accelerating the degradation of TATB. The only significant temperature difference was noticed at −10 °C, where fewer radicals formed. The radical production rates at −10 °C were some of the highest measured, however, suggesting that the rates under the other temperature conditions had slowed as a result of the extensive conversion of surface molecules to radical species. We have shown that a substantial amount of radicals can be generated with UV light, and work is ongoing to modify our EPR spectrometer so that TATB can be irradiated in the EPR cavity to measure the initial rates of radical production. This will provide information missing in this study given that our first measurements were after 4 months of irradiation. These results, as well as a computational and spectroscopic study of the identity of the radical species, will be reported in the future.

Acknowledgment. The majority of this project was funded by the Amarillo National Research Center. The authors thank

Bill Moddeman, Arnie Duncan, the NNSA's PDRD campaign, and BWXT Pantex for providing the TATB and for additional project funding. We also thank professor Gene Carlisle at West Texas A&M University for his assistance in electron paramagnetic resonance spectroscopy.

References and Notes

(1) Gibbs, T. R.; Popolato, A. *LASL Explosive Property Data*; University of California Press: Berkeley, CA, 1980.

(2) Britt, A. D.; Moniz, W. B.; Chingas, G. C.; Moore, D. W.; Heller, C. A.; Ko, C. L. *Propellants Explos.* **1981**, *6*, 94−95.

(3) Sharma, J.; Owens, F. J. *Chem. Phys. Lett.* **1979**, *61*, 2, 280−282.

(4) Sharma, J.; Garrett, W. L.; Owens, F. J.; Vogel, V. L. *J. Phys. Chem.* **1982**, *86*, 1657−1661.

(5) Firsich, D. W.; Guse, M. P. *J. Energ. Mater.* **1984**, *2*, 205−214.

(6) Wu, C. J.; Fried, L. E. *J. Phys. Chem. A* **2000**, *104*, 6447−6452.

(7) Kakar, S.; Nelson, A. J.; Treusch, R.; Heske, C.; Van Buren, T.; Jimenez, I.; Pagoria, P.; Terminello, L. J. *Phys. Rev. B* **2000**, *62*, 23, 15666−15672.

(8) Manaa, M. R.; Schmidt, R. D.; Overturf, G. E.; Watkins, B. E.; Fried, L. E.; Kolb, J. R. *Thermochim. Acta* **2002**, *384*, 85−90.

(9) Randolph, M. L. *Biological Applications of Electron Spin Resonance*; Swartz, H. M., Bolton, J. R., Borg, D. C., Eds.; Wiley-Interscience: New York, 1972.

(10) Walpole, R. E.; Myers, R. H. *Probability and Statistics for Engineers and Scientists*, 5th ed.; Prentice Hall: Englewood Cliffs, NJ, 1993.

(11) Shoemaker, D. P.; Garland C. W.; Nibler, J. W. *Experiments in Physical Chemistry*, 6th ed.; McGraw-Hill: New York, 1996.